*Progress In Electromagnetics Research B, Vol. 2, 151–164, 2008*

# NUMERICAL STUDY OF GOOS-HÄNCHEN SHIFT ON THE SURFACE OF ANISOTROPIC LEFT-HANDED MATERIALS

**W. Ding, L. Chen, and C.-H. Liang**

National Key Lab of Antenna and Microwave Technology
Xidian University
Xi'an 710071, China

**Abstract**—The Goos-Hänchen shift on the surface when an optical beam is obliquely incident from one isotropic right-handed material (RHM) into another biaxial anisotropic left-handed material (BA-LHM) is numerically studied with the finite difference time domain (FDTD) method based on the Drude dispersive models. The analytical expression of the Goos-Hänchen shift is firstly presented, moreover the condition for the existence and the sign of the Goos-Hänchen shift are also discussed. According to the theoretical analysis, several sets of constitutive parameters of BA-LHM are considered. The simulated results are in agreement with theoretical results, which validate the theoretical analysis.

## 1. INTRODUCTION

In recent studies, isotropic media with real but negativevalues of the permittivity $\varepsilon$ and permeability $\mu$ have been studied and interpreted as having a negative index of refraction. A theoretical study of such a medium was made in 1967 by Veselago [1], and the medium was labeled as a "left-handed Medium". According to his analysis, in such a "double-negative" (DNG) material, the Poynting vector of a plane wave is antiparallel with its phase velocity. In recent years, Shelby et al. [2], inspired by the work of Pendry et al. [3], constructed a composite medium in the microwave regime, by arranging arrays of small metallic wires and split ring resonators [4], and they demonstrated the negative refraction index of LHMs [5]. From then on, there has been a great deal of effort in studying the isotropic metamaterials.

Among those researches, several authors have discussed the interaction of an optical beam with the LHM surface, especially the

Goos-Hänchen shift of the beam center when it is totally reflected from the path predicted by the geometric optics consideration, due to its potential applications and rich physics. The Goos-Hänchen shift upon reflection from an surface separating an isotropic right-handed material (RHM) and an isotropic LHM has been discussed in [6–9]. In addition, some studies have been devoted to the shift in a layered structure with an isotropic LHM slab [10–13]. But up to now, the LHMs that have been prepared successfully in experiments [4, 5] are actually anisotropic in nature, and it may be very difficult to prepare an isotropic LHM [14]. Hence it is worth exploring the Goos-Hänchen shift of the optical beam totally reflected by the anisotropic LHM surface. The purpose of this paper is to study the relation between such a Goos-Hänchen shift and parameters of the biaxial anisotropic LHM (BA-LHM).

This paper mainly includes three sections: In Section 2, taking a TE polarized plane wave as an example, we deduce the dispersion relation for the plane wave in BA-LHM. In Section 3, the analytical expression of the Goos-Hänchen shift is presented when the TE polarized plane wave passes from one isotropic RHM into another BA-LHM, moreover the condition for the existence and the sign of the Goos-Hänchen shift are also discussed. In Section 4, the finite difference time domain (FDTD) method based on the Drude dispersive models [15, 16] is employed to simulate the total reflection and the Goos-Hänchen shift of the continuous-wave (CW) Gaussian Beam passing from free space into BA-LHM with several sets of constitutive parameters. The results validate the theoretical analysis.

## 2. DISPERSION RELATION IN BIAXIAL ANISOTROPIC LEFT-HANDED MATERIAL

For anisotropic materials, one or both of the permittivity and permeability are second-rank tensors. In the following we assume that both the permittivity and permeability are biaxial anisotropic with $\varepsilon$ and $\mu$ tensors that are simultaneously diagonalizable

$$\bar{\bar{\varepsilon}} = \varepsilon_0 \bar{\bar{\varepsilon}}_r = \varepsilon_0 \mathrm{diag}\left[\varepsilon_{rx}, \varepsilon_{ry}, \varepsilon_{rz}\right] = \mathrm{diag}\left[\varepsilon_x, \varepsilon_y, \varepsilon_z\right] \tag{1a}$$

$$\bar{\bar{\mu}} = \mu_0 \bar{\bar{\mu}}_r = \mu_0 \mathrm{diag}\left[\mu_{rx}, \mu_{ry}, \mu_{rz}\right] = \mathrm{diag}\left[\mu_x, \mu_y, \mu_z\right] \tag{1b}$$

where not all of the principal components have the same sign for BA-LHM.

From Maxwell's equations, all plane waves in the medium can be split into TE and TM waves, and they can be considered separately. Without losing any generality, this paper only discusses the characteristics of TE plane waves in BA-LHM. As to TM plane waves, the characteristics can be obtained through duality, by interchanging

corresponding permittivity and permeability components in Eq. (1). Now taking a TE plane wave (electric field polarized in the $+z$ direction and $k_z = 0$) as an example, the wave vector $\vec{k}$ is assumed in the $xoy$ plane, namely $\vec{k} = \vec{e}_x k_x + \vec{e}_y k_y$ and the two optical axes of BA-LHM are parallel to the coordinate axes, so the electric field can be written by

$$\vec{E} = E_0 \vec{e}_z \exp\left(ik_x x + ik_y y - i\omega t\right) \tag{2a}$$

From $\vec{k} \times \vec{E} = \omega \vec{B} = \omega \bar{\bar{\mu}} \cdot \vec{H}$, the magnetic field can be expressed as

$$\vec{H} = \left(\frac{k_y E_0}{\omega \mu_x} \vec{e}_x - \frac{k_x E_0}{\omega \mu_y} \vec{e}_y\right) \exp\left(ik_x x + ik_y y - i\omega t\right) \tag{2b}$$

Substitute Eqs. (1) and (2) into $\vec{k} \times \vec{H} = -\omega \vec{D} = -\omega \bar{\bar{\varepsilon}} \cdot \vec{E}$, then the dispersion relation of the TE wave in BA-LHM is

$$k_x^2 \Big/ \mu_y + k_y^2 \Big/ \mu_x = \omega^2 \varepsilon_z \tag{3}$$

And the time-averaged Poynting vector $\vec{S}$ and its inner product with the wave vector $\vec{k}$ can be given by

$$\vec{S} = \frac{1}{2} \mathrm{Re}\left[\vec{E} \times \vec{H}^*\right] = \mathrm{Re}\left[\frac{k_x E_0^2}{2\omega \mu_y} \vec{e}_x + \frac{k_y E_0^2}{2\omega \mu_x} \vec{e}_y\right] \tag{4}$$

$$\vec{k} \cdot \vec{S} = \frac{1}{2} \mathrm{Re}\left[\omega \varepsilon_z E_0^2\right] \tag{5}$$

From Eqs. (2) to (5) we can see that if $\mu_x \neq \mu_y$, the electric field $\vec{E}$ and magnetic field $\vec{H}$ and wave vector $\vec{k}$ cannot form a strictly left-handed triplet of vectors and the direction of energy flow cannot be in the exactly opposite direction of wave vectors, except that the wave propagation is in the direction of one of the optical axes. But if some conditions are satisfied, the TE wave can be approximately left-handed wave (i.e., $\vec{E}$, $\vec{H}$ and $\vec{k}$ form an approximately left-handed triplet of vectors and the direction of energy flow is in the backward but not exactly opposite direction of wave vector). From Eq. (5), the condition for the TE wave being approximately left-handed wave in BA-LHM is $\varepsilon_z < 0$, but other elements in Eq. (1) do not need to be negative.

## 3. GOOS-HÄNCHEN SHIFT ON THE SURFACE OF BIAXIAL ANISOTROPIC LEFT-HANDED MATERIAL

In this section we discuss the Goos-Hänchen shift on the surface when the TE polarized plane wave discussed above normal is obliquely incident from one isotropic RHM into the second BA-LHM. A schematic illustration of the system is shown in Fig. 1. The total space is divided into two regions. One is the isotropic RHM region with $\varepsilon_1 > 0$, $\mu_1 > 0$ in Region 1 ($y < 0$), the other is the BA-LHM region with permittivity and permeability tensors denoted in Eq. (1) in Region 2 ($y > 0$). The TE polarized plane wave is obliquely incident from the left lower quadrant of Region 1 into Region 2.

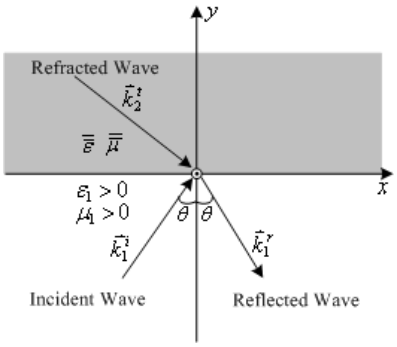


**Figure 1.** A plane wave incident from one isotropic RHM into another BA-LHM.

From Fig. 1, the wave vectors of the incident and reflected waves can be written by $\vec{k}_1^{\,i} = k_x\vec{e}_x + k_y\vec{e}_y$ and $\vec{k}_1^{\,r} = k_x\vec{e}_x - k_y\vec{e}_y$, where $k_x > 0$, $k_y > 0$. So the dispersion relation in Region 1 can be obtained

$$(k_x)^2 + (k_y)^2 = (k_1)^2 = \omega^2\varepsilon_1\mu_1 \tag{6}$$

And the electric fields of the incident and reflected waves can be obtained

$$\vec{E}_1^{\,i} = E_0\vec{e}_z \exp\left(ik_x x + ik_y y - i\omega t\right) \tag{7a}$$

$$\vec{E}_1^{\,r} = rE_0\vec{e}_z \exp\left(ik_x x - ik_y y - i\omega t\right) \tag{7b}$$

where $r$ is the reflection coefficient. From the boundary conditions of Maxwell's equations, it can be easily shown that the tangential component of the wave vector of the refracted wave $k_{2x}^t$ is equal to that of the incident wave, namely $k_{2x}^t = k_x > 0$. We can obtain the wave vector of the refracted wave $\vec{k}_2^{\,t} = k_x\vec{e}_x + k_{2y}^t\vec{e}_y$, so the electric field of the refracted wave can be expressed as

$$\vec{E}_2^{\,t} = tE_0\vec{e}_z \exp\left(ik_x x + ik_{2y}^t y - i\omega t\right) \tag{7c}$$

where $t$ is the transmission coefficient and $k_{2y}^t$ can be obtained from Eq. (3)

$$\left(k_{2y}^t\right)^2 = \omega^2 \varepsilon_z \mu_x - (\mu_x/\mu_y)\, k_x^2 \tag{8}$$

Then the magnetic fields of the incident, reflected and refracted waves can be obtained from the equation $\vec{k} \times \vec{E} = \omega \vec{B}$. Moreover the tangential components of electromagnetic fields on the surface ($y = 0$) are equal, so the reflection coefficient can be obtained

$$r = \frac{k_y \mu_x - k_{2y}^t \mu_1}{k_y \mu_x + k_{2y}^t \mu_1} = |r| \exp(i\phi) \tag{9}$$

where $|r|$ and $\phi$ are the amplitude and phase of the reflection coefficient, respectively.

It is well known that the Goos-Hänchen shift only exist when the incident wave experiences a total reflection on the surface of two media. In this paper, the $y$ component of the wave vector of the refracted wave $k_{2y}^t$ should be imaginary, then the refracted fields $E_2^t$ will attenuate exponentially in the $y$ direction from Eq. (7c) and the $y$ component of the Poynting vector of the refracted wave will be zero, namely $\vec{e}_y \cdot \vec{S}_2^t = \mathrm{Re}\left[\left(t^2 E_0^2 k_{2y}^t\right)/(2\omega\mu_x)\right] = 0$, hence no power will be transmitted into the Region 2 and the incident wave will be totally reflected. In order to keep $k_{2y}^t$ imaginary in Eq. (8), the following inequality

$$(\mu_x/\mu_y)\, k_x^2 > \omega^2 \varepsilon_z \mu_x \tag{10}$$

should be satisfied. Then $k_{2y}^t = i\sqrt{(\mu_x/\mu_y)\, k_x^2 - \omega^2 \varepsilon_z \mu_x} = i\omega\sqrt{(\mu_x/\mu_y)\, \varepsilon_1 \mu_1 \sin^2\theta - \varepsilon_z \mu_x}$ can be obtained, so the total reflection on the surface will occur and the reflection coefficient $r$ can be rewritten

$$r = \frac{k_y \mu_x - k_{2y}^t \mu_1}{k_y \mu_x + k_{2y}^t \mu_1} = \frac{\cos\theta - i\alpha}{\cos\theta + i\alpha} = \exp(i\phi) \tag{11}$$

where $\alpha = (\mu_1/\mu_x)\sqrt{(\mu_x/\mu_y)\sin^2\theta - (\varepsilon_z\mu_x)/(\varepsilon_1\mu_1)}$, $\phi = -2\arctan(\alpha/\cos\theta)$.

From the literature [17], the Goos-Hänchen shift can be calculated in terms of the phase shift of the reflection coefficient in total reflection as follow

$$d = -\frac{d\phi}{dk_x} = -\frac{\partial\phi}{\partial\theta}\frac{d\theta}{\partial k_x} = -\frac{1}{k_1 \cos\theta}\frac{\partial\phi}{\partial\theta} \tag{12}$$

After some simple algebra derivations, the Goos-Hänchen shift $d$ can be also

$$d = \frac{2\frac{(\mu_x)^2}{\mu_y}\tan\theta\left(1-\frac{\varepsilon_z\mu_y}{\varepsilon_1\mu_1}\right)}{k_1\mu_1\left[\left(\frac{\mu_x}{\mu_1}\right)^2\cos^2\theta+\frac{\mu_x}{\mu_y}\sin^2\theta-\frac{\varepsilon_z\mu_x}{\varepsilon_1\mu_1}\right]\sqrt{\frac{\mu_x}{\mu_y}\sin^2\theta-\frac{\varepsilon_z\mu_x}{\varepsilon_1\mu_1}}} \tag{13}$$

In Eq. (13), the denominator is always positive, so the sign of the Goos-Hänchen shift is determined by the following factor

$$s = \frac{1}{\mu_y}\left(1-\frac{\varepsilon_z\mu_y}{\varepsilon_1\mu_1}\right) \tag{14}$$

From the analysis in Section 1, in order to keep the TE wave be approximately left-handed wave in Region 2, $\varepsilon_z < 0$ should be satisfied but other elements in Eq. (1) do not need to be negative. In the following section, let us discuss how different combinations of the parameters in BA-LHM will affect the existence of the total reflection and the sign of Goos-Hänchen shift. Several sets of constitutive parameters of BA-LHM can be obtained which satisfy Eq. (10) and $\varepsilon_z < 0$ at the same time as follows.

CASE1: $\mu_x < 0$, $\mu_y < 0$, $\varepsilon_z < 0$

From Eq. (8), the dispersion relation of the BA-LHM satisfy a spheroid expression $k_x^2/(\mu_y\varepsilon_z)+\left(k_{2y}^t\right)^2/(\varepsilon_z\mu_x) = \omega^2$ and the inequality (10) becomes $k_x^2 > \omega^2\varepsilon_z\mu_y$. For $k_x = k_1\sin\theta = \omega\sqrt{\varepsilon_1\mu_1}\sin\theta$, so the inequality (10) can be expressed as

$$\sin\theta > \sqrt{(\varepsilon_z\mu_y)/(\varepsilon_1\mu_1)} \tag{15}$$

1) when $\varepsilon_z\mu_y \geq \varepsilon_1\mu_1$, the inequality (15) is always wrong, so the total reflection and the Goos-Hänchen shift on the isotropic-anisotropic surface never exist;

2) when $\varepsilon_z\mu_y < \varepsilon_1\mu_1$, there exists a critical angle for the incident wave, $\theta_c = \arcsin\sqrt{(\varepsilon_z\mu_y)/(\varepsilon_1\mu_1)}$. If the incident angle $\theta > \theta_c$, $k_{2y}^t$ will be imaginary and the incident wave will be totally reflected. From Eq. (14), the Goos-Hänchen shift is negative.

CASE2: $\mu_x > 0$, $\mu_y > 0$, $\varepsilon_z < 0$

In this case, the inequality (10) is always right and there will be the total reflection and the Goos-Hänchen shift for any incident angles. From Eq. (14), the Goos-Hänchen shift is positive.

CASE3: $\mu_x > 0$, $\mu_y < 0$, $\varepsilon_z < 0$

From Eq. (8), the dispersion relation of the BA-LHM satisfy a one-sheet hyperbola expression $k_x^2/(\mu_y\varepsilon_z) - \left(k_{2y}^t\right)^2/|\varepsilon_z\mu_x| = \omega^2$ and the inequality (10) becomes $k_x^2 < \omega^2\varepsilon_z\mu_y$, so the inequality (10) can be expressed as

$$\sin\theta < \sqrt{(\varepsilon_z\mu_y)/(\varepsilon_1\mu_1)} \tag{16}$$

1) when $\varepsilon_z\mu_y > \varepsilon_1\mu_1$, the inequality (16) is always right for any incident angles and the total reflection and the Goos-Hänchen shift on the isotropic-anisotropic surface always exist. From Eq. (14), the Goos-Hänchen shift is positive. Especially, when $\varepsilon_z\mu_y = \varepsilon_1\mu_1$, the inequality (16) is always right except $\theta = 90°$. Although the total reflection always exist in this case, the Goos-Hänchen shift on the isotropic-anisotropic surface is equal to zero from Eq. (14);

2) when $\varepsilon_z\mu_y < \varepsilon_1\mu_1$, there exists a critical angle for the incident wave, $\theta_c = \arcsin\sqrt{(\varepsilon_z\mu_y)/(\varepsilon_1\mu_1)}$. Different from the case 1, the total reflection and the Goos-Hänchen shift only exist when the incident angle $\theta < \theta_c$. From Eq. (14), the Goos-Hänchen shift is negative.

## 4. NUMERICAL RESULTS

In this section, the finite difference time domain (FDTD) method based on the Drude dispersive models is employed to study the total reflection and the Goos-Hänchen shift of the continuous-wave (CW) TE-polarized Gaussian Beam ($E_z, H_x, H_y$) incident from free space into BA-LHM with several sets of constitutive parameters. The principal components of the tensors in Eq. (1) can be expressed by the Drude dispersive models as follows

$$\varepsilon(\omega) = \varepsilon_0\left[1 - \frac{\omega_{pe}^2}{\omega(\omega - i\Gamma_e)}\right], \quad \mu(\omega) = \mu_0\left[1 - \frac{\omega_{pm}^2}{\omega(\omega - i\Gamma_m)}\right] \tag{17}$$

where $\omega_{pe}$, $\omega_{pm}$ are the plasma frequencies and $\Gamma_e$, $\Gamma_m$ are the collision frequencies of the electric and magnetic properties, respectively.

In the following simulations, Region 1 stands for free space with $\varepsilon_1 = \varepsilon_0$, $\mu_1 = \mu_0$, $k_1 = k_0$ and Region 2 stands for BA-LHM with $\varepsilon_z$, $\mu_x$, $\mu_y$. The $x$-$y$ FDTD space is $800 \times 400$ cells with a four-cell-layer PML absorbing boundary [18]. The cell sizes are $\Delta x = \Delta y = \lambda_0/20 = 5 \times 10^{-4}$ m, corresponding to $f_0 = 30$ GHz. The time step is chosen as $\Delta t = 0.95\Delta x/\left(\sqrt{2}c_0\right) = 1.1195$ ps. And the waist of the Gaussian Beam is $W_0 = 100\Delta x = 5 \times 10^{-2}$ m.

**4.1.** $\mu_x < 0$, $\mu_y < 0$, $\varepsilon_z < 0$

Choose $\omega_{pmx} = 2\pi\sqrt{2}f_0$, $\omega_{pmy} = \omega_{pez} = 2\pi\sqrt{(1+\sqrt{2}/2)}f_0$, and $\Gamma_e = \Gamma_m = 0$ in Eq. (17), then the parameters $\mu_x = -\mu_0$, $\mu_y = -\sqrt{2}/2\mu_0$ and $\varepsilon_z = -\sqrt{2}/2\varepsilon_0$ can be obtained and the critical angle is $\theta_c = \arcsin(\sqrt{2}/2) = 45°$. Fig. 2 presents the relation curve between the Goos-Hänchen shifts and the incident angles. From this figure, the negative Goos-Hänchen shift appears when the incident angle is greater than the critical angle. Then the incident angle $\theta_i = 55°$ is employed in the FDTD simulation. From Eq. (13), the Goos-Hänchen shift on the surface is $d = -0.01145\,\mathrm{m}$, corresponding to the FDTD cells $d = -0.01145\,\mathrm{m} \approx -23\Delta x$. Fig. 3(a) presents the electric fields ($E_z$) distributions in the whole simulation space. And the incident wave in Region 1 is indeed totally reflected when $\theta_i > \theta_c$. Fig. 3(b) presents the Gaussian Beam ($|E_z|$) and its envelope curve along the $x$ direction at $y = 200\Delta y$. From Fig. 3, the negative Goos-Hänchen shift takes place indeed and its value is approximately $-23\Delta x$, which validates the theoretical analysis.

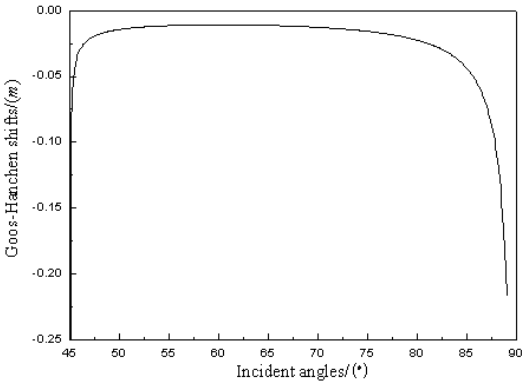


**Figure 2.** The relation curve between the Goos-Hänchen shifts and the incident angles.

**4.2.** $\mu_x > 0$, $\mu_y > 0$, $\varepsilon_z < 0$

Choose $\omega_{pmx} = 0$, $\omega_{pmy} = 2\pi\sqrt{1/2}f_0$, $\omega_{pez} = 2\pi\sqrt{2}f_0$ and $\Gamma_e = \Gamma_m = 0$ in Eq. (13), then the parameters $\mu_x = +\mu_0$, $\mu_y = +0.5\mu_0$, $\varepsilon_z = -\varepsilon_0$ can be obtained. Fig. 4 presents the relation curve between the Goos-Hänchen shifts and the incident angles. From this figure, the positive Goos-Hänchen shift appears for any incident angles. Then the incident angle $\theta_i = 50°$ is employed in the FDTD simulation. From Eq. (13), the Goos-Hänchen shift on the surface is $d = +0.00299\,\mathrm{m}$, corresponding to the FDTD cells $d = +0.00299\,\mathrm{m} \approx +6\Delta x$. Fig. 5(a) presents the electric fields ($E_z$) distributions in the whole simulation space. Fig. 5(b) presents the Gaussian Beam ($|E_z|$) and its envelope curve along the $x$ direction at $y = 200\Delta y$. From Fig. 5, the positive Goos-Hänchen shift takes place indeed and its value is approximately $+6\Delta x$,

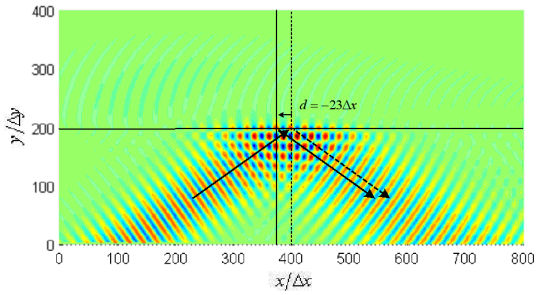


(a)

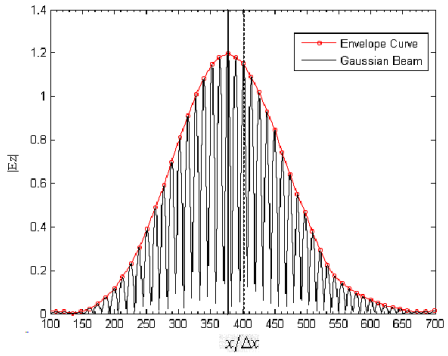


(b)

**Figure 3.** Simulation results when incident angle $\theta_i = 55°$, (a) electric fields $E_z$ distributions, (b) the Gaussian Beam $|E_z|$ and its envelope curve along the $x$ direction at $y = 200\Delta y$.

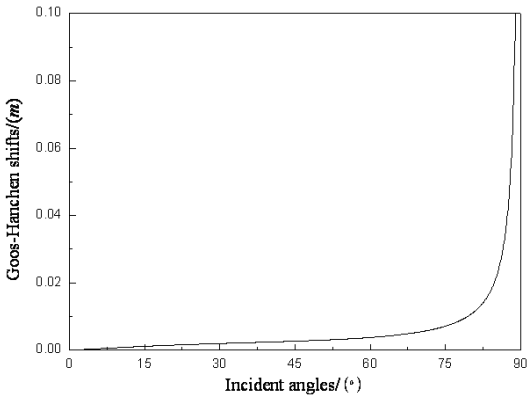


**Figure 4.** The relation curve between the Goos-Hänchen shifts and the incident angles.

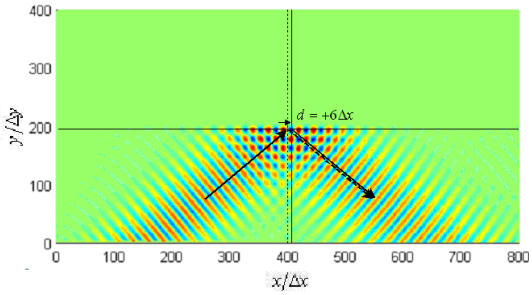


(a)

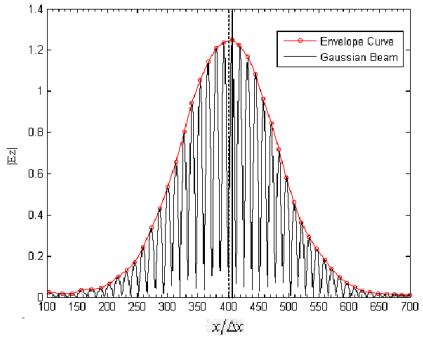


(b)

**Figure 5.** Simulation results when incident angle $\theta_i = 50°$, (a) electric fields $E_z$ distributions, (b) the Gaussian Beam $|E_z|$ and its envelope curve along the $x$ direction at $y = 200\Delta y$.

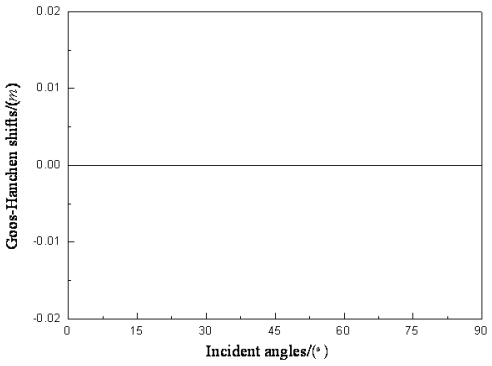


**Figure 6.** The relation curve between the Goos-Hänchen shifts and the incident angles.

which validates the theoretical analysis.

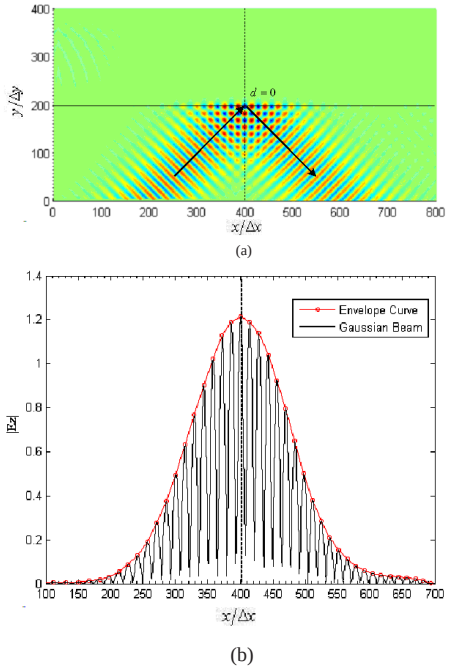


**Figure 7.** Simulation results when incident angle $\theta_i = 45°$, (a) electric fields $E_z$distributions, (b) the Gaussian Beam $|E_z|$ and its envelope curve along the $x$ direction at $y = 200\Delta y$.

### 4.3. $\mu_x > 0$, $\mu_y < 0$, $\varepsilon_z < 0$

Case1: $\mu_x = +\mu_0$, $\mu_y = -\mu_0$, $\varepsilon_z = -\varepsilon_0$

Choose $\omega_{pmx} = 0$, $\omega_{pmy} = \omega_{pez} = 2\pi\sqrt{2}f_0$ and $\Gamma_e = \Gamma_m = 0$ in Eq. (17), then the parameters above can be obtained. Fig. 6 presents the relation curve between the Goos-Hänchen shifts and the incident angles. From this figure, the Goos-Hänchen shift is always equal to zero for any incident angles because of $\varepsilon_z\mu_y = \varepsilon_1\mu_1 = \varepsilon_0\mu_0$ in Eq. (13). Then the incident angle $\theta_i = 45°$ is employed in the FDTD simulation. Fig. 7(a) presents the electric fields ($E_z$) distributions in the whole simulation space. Fig. 7(b) presents the Gaussian Beam ($|E_z|$) and its envelope curve along the $x$ direction at $y = 200\Delta y$. From Fig. 7, although the total reflection indeed takes place in this case, the Goos-Hänchen shift on the surface is zero.

Case2: $\mu_x = +\mu_0$, $\mu_y = -\sqrt{2}/2\mu_0$, $\varepsilon_z = -\sqrt{2}/2\varepsilon_0$

Choose $\omega_{pmx} = 0$, $\omega_{pmy} = \omega_{pez} = 2\pi\sqrt{(1+\sqrt{2}/2)}f_0$ and $\Gamma_e = \Gamma_m = 0$ in Eq. (17), then the parameters above can be obtained and the critical angle is $\theta_c = \arcsin(\sqrt{2}/2) = 45°$. Fig. 8 presents the relation curve between the Goos-Hänchen shifts and the incident angles. From this figure, the negative Goos-Hänchen shift appears when the incident angle is less than the critical angle. Then the incident angle $\theta_i = 40°$ is employed in the FDTD simulation. From Eq. (13), the Goos-Hänchen shift on the surface is $d = -0.0076\,\mathrm{m}$, corresponding to the FDTD cells $d = -0.0076\,\mathrm{m} \approx -15\Delta x$. Fig. 9(a) presents the electric fields

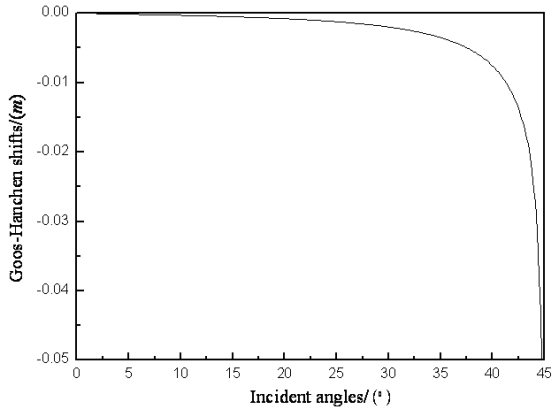


**Figure 8.** The relation curve between the Goos-Hänchen shifts and the incident angles.

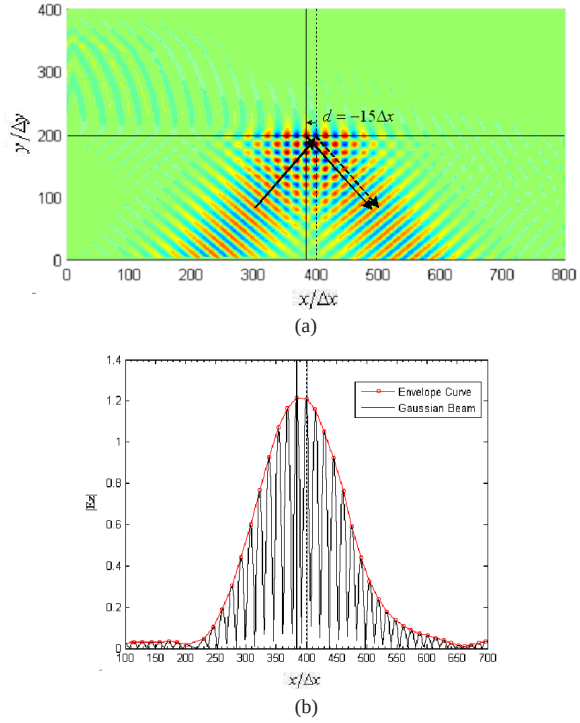


**Figure 9.** Simulation results when incident angle $\theta_i = 40°$, (a) electric fields $E_z$ distributions, (b) the Gaussian Beam $|E_z|$ and its envelope curve along the $x$ direction at $y = 200\Delta y$.

($E_z$) distributions in the whole simulation space. And the incident wave in Region 1 is indeed totally reflected when $\theta_i < \theta_c$, which is quite different from the case of two isotropic RHMs and the case of 4.1. Fig. 9(b) presents the Gaussian Beam ($|E_z|$) and its envelope curve along the $x$ direction at $y = 200\Delta y$. From Fig. 9, the negative Goos-Hänchen shift takes place indeed and its value is approximately $-15\Delta x$, which validates the theoretical analysis.

## 5. CONCLUSION

This paper has analyzed the Goos-Hänchen shift on the surface of BA-LHM theoretically and numerically. The condition for the existence of total reflection and the relationship between the Goos-Hänchen shift and the parameters of BA-LHM have been discussed in detail when the TE polarized plane wave is obliquely incident from one isotropic RHM into another BA-LHM. Meanwhile the corresponding numerical results by FDTD based on the Drude dispersive models are presented with different sets of constitutive parameters of BA-LHM. The simulated results are in agreement with theoretical analysis, which will be helpful for the studies on the electromagnetic characteristics of anisotropic LHMs further.

## REFERENCES

1. Veselago, V. G., "The electrodynamics of substances with simultaneously negative values of $\varepsilon$ and $\mu$," *Sov. Phys. Usp.*, Vol. 10, 509–515, 1968.
2. Pendry, J. P., A. J. Holden, D. J. Robbins, and W. J. Stewart, "Low frequency plasmons in thin-wire structures," *J. Phys. Condens. Matter.*, Vol. 10, 4785–4809, 1998.
3. Pendry, J. P., A. J. Holden, D. J. Robbins, and W. J. Stewart, "Magnetism from conductors and enhanced nonlinear phenomena," *IEEE Trans. Microwave Theory Tech.*, Vol. 47, 2075–2084, 1999.
4. Smith, D. R., W. J. Padilla, D. C. Vier, S. C. Nemat-Nassser, and S. Schultz, "Composite medium with simultaneously negative permeability and permittivity," *Phys. Rev. Lett.*, Vol. 84, 4184–4187, 2000.
5. Shelby, R. A., D. R. Smith, and S. Schultz, "Experimental verification of a negative index of refraction," *Science*, Vol. 292, 77–79, 2001.

6. Berman, P. R., "Goos-Hänchen shift in negatively refractive media," *Phys. Rev. E*, Vol. 66, 067603, 2002.
7. Lakhtakia, A., "On planewave remittances and Goos-Hänchen shifts of planar slabs with negative real permittivity and permeability," *Electromagnetics*, Vol. 23, 71–76, 2003.
8. Lakhtakia, A., "Positive and negative Goos-Hänchen shifts and negative phase-velocity mediums (alias left-handed materials)," *Int. J. Electron. Commun.*, Vol. 58, 229–231, 2004.
9. Qing, D. K. and G. Chen, "Goos-Hänchen shifts at the interfaces between left- and right-handed media," *Opt. Lett.*, Vol. 29, 872–874, 2004.
10. Li, C. F., "Negative lateral shift of a light beam transmitted through a dielectric slab and interaction of boundary effects," *Phys. Rev. Lett.*, Vol. 91, 133903, 2003.
11. Shadrivov, I. V., A. A. Zharov, and Y. S. Kivshar, "Giant Goos-Hänchen effect at the reflection from left-handed metamaterials," *Appl. Phys. Lett.*, Vol. 83, 2713–2715, 2003.
12. Shadrivov, I. V., R. W. Ziolkowski, A. A. Zharov, and Y. S. Kivshar, "Excitation of guided waves in layered structures with negative refraction," *Opt. Express*, Vol. 13, 481–492, 2005.
13. Wang, L. G. and S. Y. Zhu, "Large negative lateral shifts from the Kretschmann-Raether configuration with left-handed materials," *Appl. Phys. Lett.*, Vol. 87, 221102, 2005.
14. Hu, L. B and S. T. Chui, "Characteristics of electromagnetic wave propagation in uniaxially anisotropic left-handed materials," *Phys. Rev. B*, Vol. 66, 085108: 1–7, 2002.
15. Ziolkowski, R. W. and E. Heyman, "Wave propagation in media having negative permittivity and permeability," *Phys. Rev. E*, Vol. 64, 056625, 2001.
16. Ziolkowski, R. W., "Pulsed and CW Gaussian beam interactions with double negative metamaterial slabs," *Opt. Express*, Vol. 11, 662–681, 2003.
17. Artmann, K., "Berechnung der Seitenversetzung des totalreflektierten Stranles," *Ann. Physik*, Vol. 2, 87–102, 1948.
18. Cummer, S. A., "Perfectly matched layer behavior in negative refractive index materials," *IEEE Antennas and Wireless Propagation Letters*, Vol. 3, 2004.